

# Combined dielectrophoretic and impedance system for on-chip controlled bacteria concentration: application to Escherichia Coli.

Beatriz del Moral-Zamora<sup>\*1</sup>, Jaime Punter-Villagrassa<sup>\*1</sup>, Ana M. Oliva-Brañas<sup>2</sup>, Juan Manuel Álvarez-Azpeitia<sup>2</sup>, Jordi Colomer-Farrarons<sup>1</sup>, Josep Samitier<sup>1,2,3</sup>, Antoni Homs-Corbera<sup>1,2,3</sup>, and Pere Ll. Miribel-Català<sup>1</sup>

<sup>1</sup> Department of Electronics, University of Barcelona, Martí i Franquès 1, 08028, Barcelona, Spain.

<sup>2</sup> Nanobioengineering group, Institute for Bioengineering of Catalonia (IBEC), Baldiri Reixac 10-12, 08028, Barcelona, Spain.

<sup>3</sup> Centro de Investigación Biomédica en Red en Bioingeniería, Biomateriales y Nanomedicina (CIBER-BBN), Spain.

**Abbreviations:** Impedance analysis (IA), escherichia coli (*E. coli*), digital lock-in (DLIA), analog-to-digital converter (ADC), finite element method (FEM).

**Correspondent author:** Jaime Punter-Villagrassa Department of Electronics, University of Barcelona, Martí i Franquès 1, 08028, Barcelona, Spain. [jpunter@el.ub.edu](mailto:jpunter@el.ub.edu)

**Keywords:** Autonomous Device; Bacteria Concentrator; Dielectrophoresis; Escherichia Coli; Impedance Analysis.

6825 words.

## Abstract

The present paper reports a bacteria autonomous controlled concentrator prototype with a user-friendly interface for bench-top applications. It is based on a micro-fluidic lab-on-a-chip and its associated custom instrumentation, which consists in a dielectrophoretic actuator, to pre-concentrate the sample, and an impedance analyser, to measure concentrated bacteria levels. The system is composed by a single micro-fluidic chamber with interdigitated electrodes and custom electronics instrumentation. The prototype is supported by a real-time platform connected to a remote computer which automatically controls the system and displays impedance data which is used to monitor bacteria accumulation status on-chip. The system automates the whole concentrating operation. Performance has been studied for controlled volumes of *Escherichia Coli* (*E. coli*) samples injected into the micro-fluidic chip at constant flow rate of 10  $\mu\text{l}/\text{min}$ . A media conductivity correcting protocol has been developed, as so as the preliminary results shown the distortion of impedance analyser measurement produced by bacterial media conductivity variations through time. With the correcting protocol, the measured impedance values were related to the quantity of bacteria concentrated with a correlation of 0.988 and a coefficient of variation of 3.1%. Feasibility of *E. coli* on-chip automated concentration, using the miniaturized system, has been demonstrated and impedance monitoring protocol adjusted and optimized, to handle electrical properties changes of the bacteria media over time.

## 1. Introduction

In the last few years, the electrical properties of cells and pathogens have been used to explore new methods of manipulation and characterization, such as dielectrophoresis (DEP) [1], or impedance analysis (IA) [2, 3]. For instance, DEP has been recently used to control embryonic stem cells to form embryoid bodies in shorter time[4] and H.O. Fatoyinbo et al [5] have measured biophysical parameters of cells (cytoplasmic conductivity, membrane conductivity and cell wall conductivity) by analysing its cells DEP behaviour. Moreover, IA was also advantageous to detect ovarian cancer cells SKV3[6] or to detect insulin levels in blood serum [7] so as to predict diabetes or trauma. Here we present a specific, miniaturized and compact equipment solution to a fully automated and controlled bacteria concentration device.

Bacterium concentration is a time consuming procedure in a laboratory since it involves culture processes [8,9] to obtain a significant sample. This could be improved by using DEP, which refers to the force experienced by a particle inside a non-uniform electric field [10, 11], since cells could be concentrated in-chip in few minutes. DEP is a convenient and rather selective handling method that has been applied in many biological fields and especially in lab-on-a-chip (LoC) devices [12–14] . An example of this is the work reported by Lapizco-Encinas et al. (2004) [15] where several types of bacteria in water were concentrated and separated by DEP combined with insulator-based structures (called iDEP), or in the paper presented by Braff et al. (2012) [16] where bacteria were successfully DEP trapped in poly(methyl methacrylate) PMMA structures. Also, its selectivity was reported as a benefit for sample preparation, since allows to isolate the desired cell or pathogen in different applications [17–19]. Moon et al. (2011) [19] use DEP to separate and detect circulating tumor cells (CTCs), whose size and resistance to filtering shear stress are likely to be significant variables, from blood cells. This becomes also an advantage in case of environmental samples, where soil particles with same bacteria size are also present and couldn't be eliminated by filtration or centrifugation. This has been also solved by using DEP [20], taking profit of its selectivity by cell electrical properties. Hence, we used DEP in here applied for concentration purposes.

Moreover, pathogenic bacteria detection protocols are expensive in terms of equipment and time, typically requiring different equipment and several days to obtain results [21, 22]. Techniques like pathogenic-specific antibody coated magnetic beads [23, 24] or hybridization of DNA fragments of bacteria [25], improves the analysis time, but still needs complex equipment and takes several hours to carry out. This could be improved by using IA. Impedance frequency dependence, which is related to the electrical conductivity and permittivity properties of the material, was reported as an effective solution to characterization of cells and their behaviour, also in LoC devices [26]. In fact, some publications have reported the use of IA technique to control bacterial growth or to detect its presence [27]. One example of such work is the paper

presented by Dweik et al (2012) [28], where bacterial presence was rapidly detected measuring the antibody/antigen bonding by IA between 100 Hz and 10 MHz. Also, in the work developed by Grossi et al. (2012) [29], the quantity of bacteria during a culture process was detected by impedance measured at 200 Hz sinusoidal with a 100mV peak-to-peak signal.

The combination of DEP and IA [3,30] in a single equipment together with a single micro-fluidic chip becomes a practical bench-top device. In the last years have been presented several biosensors and applications aiming for the successful combination of both technique. Hamada et al. (2013) [3] presented a bacterial detection device combining both positive and negative DEP with dielectrophoretic impedance measurement (DEPIM). The biosensor relay on a pair of inter-digitated electrodes (IDE) for separately DEP concentration and DEPIM measurement, while using commercial devices to operate the application. The cellular solution conductivity variations through time, which affects the impedance measurement, has not been considered, and the measurement instability produced by the magnitude of DEP voltage has been reported. Dastider et al. (2013) [30] have designed an impedance biosensor for the specific detection of *Escherichia Coli* (*E. coli*) O157:H7 combining DEP and IA techniques at slow flow rate of 2 $\mu$ l/min. This application has different IDE for cellular separation and detection purposes. The cellular detection IDE has been functionalized with polyclonal anti-*E. coli* antibodies for specific detection of *E. coli* O150:H7, removing versatility of the device. Moreover, the presented results for cellular concentration detection, based on impedance measurements, have not considered the cellular solution conductivity variations, as well as the influence of DEP voltages on the impedance measurement.

Our work presents a totally custom equipment for quick and easy way to concentrate bacteria with DEP technique at relatively high flow rates [31, 32], while monitoring its concentration by means of IA technique in a real-time scenario. The presented equipment addresses the issues associated with the combination of these techniques, as well as present a simpler biosensor and custom electronics instrumentation for a future integration of the whole system on a Lab-on-a-Chip (LoC) device. The device, with its main components, is presented in Fig. 1.

The device is composed of a customized electronic module. The sample is pre-concentrated through DEP generation and bacteria concentration measured through sample IA monitoring, with a four-electrode sensor topology, on a single micro-fluidic chamber. The electronic module is supported by a real-time platform for a continuous concentration monitoring, connected to a remote computer through a standard Ethernet connection, which enables the system configuration and data display. First, it allows automated functionalities, such as multiplexing signals between the DEP generator and the IA analyzer in the micro-fluidic chip, in order to avoid DEP voltages disturbance of IA measurement, and auto-scale of the electronic instrumentation gains when necessary, for better signal acquisition. Second, it is connected to a

remote computer with a user-friendly front-end user panel, where the system user can configure the experiment variables, such as measurement time for signal multiplexing, signal operation frequency and output gain, while displaying the impedance measurements related to actual bacteria concentration level.

The solution presented controls, in an automated way, the bacteria concentration and monitoring process, and has been validated for a seriously pathogenic bacterium like *E. coli*, pathogenic variants of which cause morbidity and mortality worldwide [33], and is therefore a topic of interest. *E. coli* has been reported as one of the main antimicrobial resistant pathogens for healthcare-associated infections reported to the National Healthcare Safety Network [34], being the primary cause of widespread pathologies such as significant diarrheal and extra-intestinal diseases [33] or urinary tract infections [35]. Furthermore, *E. coli* can be found as a bacterial food contamination [21] and causes avian coli-bacillosis, one of the major bacterial diseases in the poultry industry and the most common avian disease communicable to humans [36].

The aims of the study presented were (I) to prove the feasibility of DEP generator and IA analysis combination for controlled concentration using a single equipment together with a single micro-fluidic chip; (II) to establish a protocol for autonomous concentration procedure; and (III) to develop a complete electronic equipment with an electronic instrumentation, embedded software control and user interface for a complete autonomous and reliable bacteria concentrator device, based on DEP generator and IA technique.

This novel, specific device has been proven as a robust and reliable automated system and protocol for bacteria controlled concentration. It will provide the scientific community with a rapid tool for bacteria presence detection, by avoiding previous slow preparations in pre-concentration and culture processes, reducing procedure times for a faster diagnosis and treatment.

## 2. Theory

### 2.1. The dielectrophoretic effect

Dielectrophoresis [11] defines the movement of an electrically neutral particle when a non-uniform electric field is applied. If the particle is considered homogeneous and isotropic and is polarized linearly, then the dielectrophoretic force is defined by (1) [37,38], where  $V$  is the volume of the particle,  $E$  is the electric field, and  $\alpha$  is the effective polarizability, which is defined by the expression (2):

$$F_{DEP} = \frac{1}{2} V \cdot \text{Re} \alpha^* \omega \nabla E^2 \quad (1)$$

$$\alpha = 3\epsilon_0\epsilon_m F_{CM} \quad (2)$$

where  $\varepsilon_0$  and  $\varepsilon_m$  are the vacuum permittivity and the medium permittivity respectively and  $F_{CM}$  is the Clausius-Mosotti Factor. The  $F_{CM}$  sign describes the force direction: if  $F_{CM}$  is positive, the particle is attracted to an electrical field maximum (which is called positive DEP or p-DEP) and if negative, to an electrical field minimum (negative DEP or n-DEP). Hence, the DEP force allows control of the movement of a particle by varying the applied signal, by changing the electrode shape, by placing dielectric structures or by modifying media properties. Here we used a pair of inter-digitated gold electrodes to pre-concentrate *E. coli* cells. In order to define the suitable trapping frequency, an *E. coli* geometry model is considered. This bacterium is approximated to an ellipsoid shape with two dielectric layers [10], which modifies the Clausius – Mosotti factor expression:

$$F_{CM_i} \omega = \frac{1}{2} \frac{\varepsilon_p^* - \varepsilon_m^*}{\varepsilon_m^* + A_i \varepsilon_p^* - \varepsilon_m^*} \quad (3)$$

where  $\varepsilon_m$  is the medium permittivity,  $\varepsilon_p$  is the particle permittivity and  $A_i$  is the depolarization factor of an individual ellipsoid axe ( $i = x, y, z$ ), where  $e$  is the eccentricity that involves the ellipsoid dimensions (where ‘ $b$ ’ is the height and ‘ $a$ ’ the width):

$$A_x = \frac{1-e^2}{2e^3} \log \left( 1 + \frac{e}{1-e-2e} \right) \quad (4)$$

$$A_z = A_y = \frac{1-A_x}{2} \quad (5)$$

$$e = \sqrt{1 - \frac{b^2}{a^2}} \quad (6)$$

The representation of expression (3) showed that the optimal frequency to manipulate *E. coli* cells by p-DEP is at 1 MHz as we perfectly know by previous studies of the group [39, 40]. This frequency was therefore chosen for the pre-concentrating stage.

## 2.2. Impedance and available measurement methods

The bioimpedance [41, 42] can be measured as the voltage response of a biological material to the application of a current bias signal, and is defined by the Ohm’s law. The methods of impedance measurement are classified by the number of electrodes used: 2, 3 or 4 electrode method. The difference between methods resides in how bias current signal is applied and how the sensor voltage signal response is read.

A 2 electrode configuration is the basic topology, defined by the working electrode, where bias signal is applied, and the reference electrode, which tracks the bias current signal and provides a reference for the voltage measurement. However, as the current bias signal flows through the reference electrode, this topology entails some problematic behaviour as the voltage reference is distorted due to electrode polarization. In order to avoid this effect, the 3 electrode topology

adds a third electrode to supply the bias current signal, while the reference electrode remains as a voltage reference.

Although this is an improvement, the impedance measurement with this topology can be distorted due to the working electrode impedance polarization, as the current bias signal is directly applied where the single-ended voltage measurement signal is read. In this paper, the 4 electrode method was used (Fig. 2.A, electrodes ER1, ER2, ECI1, ECI2), which was composed of two current injection electrodes and two voltage reading electrodes, as this electrode topology avoids electrode polarization distortion in impedance measurement due to a complete differential voltage measurement [43].

### **3. Material and methods**

#### **3.1 Micro-fluidic chip design and fabrication**

The designed micro-fluidic chip design is showed in Fig. 2.B. This had two inter-digitated electrodes, which were shared between the dielectrophoresis generator and impedance analyzer readout electronics, and 2 lateral electrodes, which were used to inject the necessary current so as to obtain the impedance measure. The inter-digitated electrodes were formed by 40 pairs of 6 mm x 50  $\mu$ m electrodes separated by 50  $\mu$ m. The lateral electrodes (6 mm x 300  $\mu$ m) were separated by 200  $\mu$ m from the inter-digitated ones. These electrodes were attached to a PDMS micro-fluidic chamber with a volume of 4.8  $\mu$ l. The fabrication of the micro-fluidic chips followed a protocol based on three main steps: micro-channel moulding, electrode fabrication, and micro-fluidic chip bonding.

First, SU8 50 (MicroChem™) masters were fabricated over glass slides (Deltalab™) and Polydimethylsiloxane (PDMS) replicas were created. In order to do this, the glass slide was cleaned and activated by Piranha attack for 15 minutes. Then a 50- $\mu$ m high SU-8 50 (MicroChem™) was spun over the slides. They were later exposed and developed so as to obtain the desired micro-channels. Afterwards, a 10:1 ratio of PDMS pre-polymeric solution (Dow Corning™ Sylgard®184) was mixed, degassed and poured into the mould to replicate the microchannels. Finally, the PDMS was cured at 70°C for 1 h and peeled from the master.

Secondly, in order to fabricate the microelectrodes over a set of the LoC sealing glass slides (Deltalab™), a lift-off soft lithographic process was used. AZ 1512 (AZ Electronic Materials™) photoresist was chosen as a sacrificial layer in this process. First, a Piranha cleaning procedure was performed over the glass slides. Later, AZ 1512 was spun on these slides, exposed and developed. Then, two metal layers, 20 nm of Ti and 80 nm of gold, were vapour-deposited sequentially. The electrode structures were finally obtained by removing the AZ photo-resist.

As a final micro-fluidic chip fabrication step, once the PDMS replica and the microelectrodes were finished, both parts were assembled to create a sealed structure. First, the surfaces were cleaned using an oxygen plasma process. Hereinafter, the PDMS channels were aligned and attached to the glass substrate. Later, cables were welded to each electrode pad using conductive silver paint and mechanically strengthened using an epoxy glue mix, later cured at room temperature for 60 minutes. Finally, two NanoPort Assemblies were attached in order to set the inlet and outlet fluidic connections.

### 3.2. Combined DEP and IA device

#### 3.2.1 Dielectrophoretic signal generator electronics

The designed dielectrophoretic signal generator module is presented in Fig. 3. Four channels with different phases ( $0^\circ$ ,  $90^\circ$ ,  $180^\circ$ ,  $270^\circ$ ), which could be connected in different ways to the electrodes DEP1 and DEP2, were defined so as to add versatility to the board in dielectrophoretic terms. Each channel generates a sinusoidal signal at 1 MHz with variable output voltage from 1 to 15 V<sub>pp</sub> (peak-to-peak) to control the DEP force intensity, and is composed of three modules: a) A square signal generator that provides four shifted and frequency stable signals (A). b) A power driver which boost the signal from the previous module so as to activate the following stage (B). c) A Class E Amplifier, which generated the DEP sinusoidal signal (C).

The first module, the square signal generator, is based on the LTC6902 (Linear Technology). The synchronized outputs are shifted  $\phi_1=0^\circ$ ,  $\phi_2=90^\circ$ ,  $\phi_3=180^\circ$  and  $\phi_4=270^\circ$  respectively. Their output frequency is selectable by an external resistor ( $R_{SET}$ ), following the equation 7 where ( $N = 10$  is related to frequency working range and  $M = 4$  is the number of active outputs),

$$f_{out} = \frac{10 \text{ MHz}}{N \cdot M} \cdot \frac{20 \text{ k}\Omega}{R_{set}} \quad (7)$$

LTC6902 outputs have a supplying limit of 400  $\mu$ A. Hence, a power driver is used to increase the current capabilities. An UCC27424 (Texas Instruments) is chosen for this purpose. This device boosts the current levels of the input signal up to 4 A, which is sufficient current to drive the final module. This module is a Class E Amplifier that generates the necessary sinusoidal signals to apply DEP. This amplifier configuration generates high frequency signals with stable output voltages [44,45,46] by injecting a square high current control signal.

The Class E amplifier is composed of an inductor  $L_e$ , a capacitor  $C_e$  and a resonance tank formed by the inductor  $L$  and the capacitor  $C$ . The L-C tank generates a 1 MHz sinusoidal signal by using the 1 MHz square signal from the previous modules. The circuit parameters ( $L_e$ ,  $C_e$ ,  $C$ ,  $L$ ) were configured in function of the necessary output frequency, the output impedance



and the equivalent resistance of the micro-fluidic chip. Thus, four independent channels perfectly synchronized at  $\phi_1$ ,  $\phi_2$ ,  $\phi_3$  and  $\phi_4$  are obtained.

### 3.2.2. Impedance Analyzer Electronics

A fully customized electronic circuit was specifically designed to carry out the IA experiments. As previously stated, the micro-fluidic device impedance measurement is based on the 4 electrode topology. A 4 electrode method is composed of two Current Injection (ECI1 and ECI2) electrodes and two voltage Reading (ER1 and ER2) electrodes. The main advantage of this system is that electrode impedances are cancelled, obtaining a more reliable measure.

The circuit specifications were defined taking into account the sample media impedance, and considering the micro-fluidic device characteristics and the frequency ranges where bacterium could be discriminated [47,48].

The impedance analyzer architecture consists of two modules: the Current Injection module (CI in Fig. 4.B) that provides a frequency configurable voltage sinus signal ( $V_{RS}$ ) that is converted to a current signal (voltage-to-current converter circuit) to bias/drive the Current Injection electrodes ECI1 and ECI2. An Instrumentation Amplifier (IA) senses the differential voltage between the Reading electrodes ER1 and ER2 ( $V_{IS}$ ).

The second module, Signal Digitalization and Post-Processing (SDPP in Fig. 4.A), calculates the impedance measurement through the voltage signals provided by the previous stage, and automatically controls the hardware configuration. This module is composed of a real time platform sbRIO9632 (National Instruments) with an embedded software for data processing and hardware control. A signal conditioning stage converts voltage signals from a bi-polar single-ended to a uni-polar differential signal to be processed by an analog-to-digital converter (ADC). The first module (CI), Current Injection, is based on a signal generator AD9833 (Analog Devices) and a voltage to current converter. The signal generator AD9833 provides a stable voltage signal with a wide variable frequency range, 0 MHz to 12.5 MHz, which is controlled by an SPI communication protocol. The voltage to current converter is a modified Howland cell based on AD8066 (Analog Devices) operational amplifiers (OA1 and OA2) which guarantee a wide bandwidth and a high slew-rate while maintaining a low spectral noise and a low offset performance. The Howland cell uses  $R_{SET}$  and the Reference Signal ( $V_{RS}$ ) amplitude to define a stable current signal ( $I_{OUT}$ ) at the output of the circuit (8) regardless the connected load.

$$I_{OUT} = \frac{1}{R_{SET}} V_{RS} \quad (8)$$

The differential voltage between ER1 and ER2 electrodes is acquired by means of the instrumentation amplifier (IA) INA163 (Texas Instruments) which allows a wide bandwidth

with a low spectral noise and low Total Harmonic Distortion. The measured voltage (signal  $V_{IS}$ ) is related to the differential voltage between the reading electrodes (ER1 and ER2),  $G$  being the instrumentation amplifier gain. This  $V_{IS}$  signal is then adapted and processed by the SDPPM module in order to extract the impedance of the media.

$$V_{IS} = G \cdot V_{ER1} - V_{ER2} \quad (9)$$

The second module (SDPP), Signal Digitalization and Post-Processing, consists in a 12-bit, dual, low power analogue to digital converter ADC12D040 (ADC) (Texas Instruments), capable of converting both analogue input signals at 40 MSPS simultaneously. 12-bit resolution does not represent a significant drawback in the final system resolution, as  $V_{RS}$  is scaled to the full range ADC analogue input and the system provides a real time gain auto-scale for the instrumentation amplifier gain  $G$ . The analogue inputs are converted from single ended to differential with a differential amplifier (DA) AD8138 (Analog Devices), with a high slew rate with low distortion and input noise. The impedance measurement is carried out with a digital lock-in (DLIA) based on the Frequency Response Analyzer (FRA) approach [49]. The FRA is a real-time mathematical processing system, embedded in the 400 MHz microprocessor from the real time platform sbRIO9632, which adopts sine and cosine signals related to  $V_{RS}$ , and by means of two multipliers and a filter stage, the real ( $V_{REAL}$ ) and imaginary ( $V_{IM}$ ) components values (10) of the measured signal  $V_{IS}$  are obtained (Fig. 4.C.). The key measurement in our work is the impedance magnitude ( $|Z_{CELL}|$ )(11). This value is calculated based on the  $V_{REAL}$  and  $V_{IM}$  components.

$$V_{REAL} = \frac{1}{2V_{RS}} \cdot V_{IS} \cdot \cos(\varphi_{IS}); V_{IM} = \frac{1}{2V_{RS}} \cdot V_{IS} \cdot \sin(\varphi_{IS}) \quad (10)$$

$$Z_{CELL} = \frac{\sqrt{V_{REAL}^2 + V_{IM}^2}}{V_{RS}} \cdot R_{SET} \quad (11)$$

For accurate hardware control, the real time platform sbRIO9632 has a FPGA Spartan-3 (Xilinx), which allows us to provide steady clock signals, needed on the instrumentation, which can be automatically adjusted, allowing complete real-time control of the chip electrodes multiplexing. As stated in section 2.1, the micro-fluidic chip had two inter-digitated electrodes, which were shared between the DEP generator and the IA readout electronics. When an IA measurement was done the DEP generator was disconnected, suspending the trapping process. If this process was not properly timed, already trapped bacteria would be lost in the process, so the real-time control allowed an optimized timing process minimizing the bacteria loss. Moreover, the disconnection of DEP voltage signals contributes to a better bacterial concentration monitoring avoiding distortion and instability on the IA measurement. The impedance analysis process had been programmed and tested to last for a period of the applied

current signal, plus 1 ms for multiplexor switching times and stabilization. In addition, real-time platform allows complete parallel signal acquisition for all the frequency ranges, and the development of an embedded hardware control, such as  $R_{SET}$  multiplexed auto-scale, instrumentation amplifier gain  $G$  auto-scale and signal generator automatic frequency sweep. This real-time embedded hardware control represents the basic features of an automated and complete FRA approach. The real-time platform allows the system configuration and data display, with a user-friendly front-end user panel (Fig. 4.C), by means of an external computer connected to the platform with a standard Ethernet connection.

### 3.3 Bacteria culture

A laboratory sample formed by *E.coli* 5K strains (Genotypes: F<sup>-</sup>, hdsR, hdsM, thr, thi, leu, lacZ) were grown overnight in 10 mL of Luria–Bertani (LB) broth at 37 °C. The achieved cell concentration (estimated by performing viable cell counts in LB agar) was  $10^9$  cells/mL. Then, the *E. coli* culture was pelleted by centrifugation at 5000 rpm for 5 minutes. Bacteria were then re-suspended in 10 mL of deionized water. Finally, the samples were diluted (final concentration of  $2 \cdot 10^7$  cells/mL) and frozen in 1 mL collecting tubes for storage purposes.

### 3.4 Conductivity measurements

As *E. coli* concentration was measured by means of impedance analysis, bacteria samples conductivity was monitored while in tube, a major factor in impedance analysis reliability, using a commercial bench top conductivity meter Corning 441. Prior to the experiments, bacteria samples were diluted in de-ionized water with a conductivity of  $8.2 \cdot 10^{-5}$  S/m, but the conductivity of the samples at the time of the experiment, after the process of storage and thawing, was subject to variations. A sample conductivity analysis had to be done at the beginning of the experiment. The conductivity meter probe was calibrated and introduced into the 1 mL collecting tubes until it was totally covered by the bacteria sample.

### 3.5 Experimental setup

The micro-fluidic chip was placed over an inverted microscope stage (Olympus™ IX71) connected to a digital camera (Hamamatsu™ Orca R2). Moreover, the micro-fluidic chip was connected to a 6-port manual valve (Valco™). This valve was also connected to a 5-mL syringe filled with de-ionized water ( $8.2 \cdot 10^{-5}$  S/m) and placed on an infusion micro-pump (Cetoni™ NEMESYS) so as to obtain a continuous flow rate. The micro-fluidic chip's gold electrodes were connected to the custom combined DEP and IA device.

#### 4. Results and discussion

The designed combined device was validated by a series of *E. coli* concentration and impedance measurement tests. First of all, so as to validate the system as an autonomous bacteria concentrator, and study the effect of real-time monitoring by means of IA measurement, *E. coli* was continuously injected through the valve to the micro-fluidic chip at a 5  $\mu\text{L}/\text{min}$  flow rate, and pre-concentrated by DEP by two counter-phased signals of 15Vpp. In addition, the impedance module was programmed to proceed with a 3 milliseconds impedance measurement every 30 seconds meanwhile DEP module was continuously trapping bacteria. As a first approach, the conductivity of the solution has not been corrected to study the effect its variations over time on the IA measurement. Different tests for different applied current signal frequencies were done. Taking into consideration the electronics and micro-fluidic chip design, impedance measurement was performed at continuous alternating current of 10  $\mu\text{A}$  in the 500 Hz to 5 kHz frequency range, where bacterium could be discriminated [47,48] and evaluated using 100 Hz spaced sampling intervals.

The measured bioimpedance ( $|Z|$ ), depicted in Fig.5.A., clearly shows a decreased impedance as the trapped bacteria concentration increases, regardless of the frequency.

This behaviour was clearly explained by the conductivity changes taking place in bacteria samples over time. Measured conductivity was recorded periodically in-tube during the experiments showing a rise from  $0.5 \cdot 10^{-3} \text{ S/m}$  to  $2.5 \cdot 10^{-3} \text{ S/m}$  until it stabilized. This conductivity change, related to the original sample prior to the trapping process, may be translated into a theoretical variation in impedance. This estimated impedance, related to measured bacteria sample in-tube conductivity, was calculated considering the micro-fluidic chip electrodes' geometric characteristics. In Fig.5.B. impedance variation ( $\Delta|Z|$ ) through time for the measured on-chip impedance, during the trapping process, and for the estimated on-tube impedance are shown.

Results show a very similar behaviour through time of both measurements. Acquired data variations through time for the first 40 minutes, before conductivity stabilization, were -52.41  $\Omega/\text{min}$  for measured impedance and -54.79  $\Omega/\text{min}$  for conductivity related impedance, which confirms that the first impedance measurements are related to bacteria sample conductivity rather than trapped bacteria concentration, underlining the need for a media conductivity correcting protocol.

A 2-D finite element method (FEM)-based study with Multiphysics software (Comsol) further shows the dominating effect of sample conductivity changes on the bioimpedance measurements when left uncontrolled. *E. coli* 5K physical and electrical properties were defined for the different model layers ( $\sigma_{\text{wall}} = 0.68 \text{ S/m}$ ,  $\epsilon_{\text{r\_wall}} = 74$ ,  $\sigma_{\text{membrane}} = 5 \times 10^{-8} \text{ S/m}$ ,  $\epsilon_{\text{r\_membrane}} = 9.5$ ,  $\sigma_{\text{cytoplasm}} = 0.19 \text{ S/m}$ ,  $\epsilon_{\text{r\_cytoplasm}} = 49.8$ ). Then different medium conductivities were defined, as well

as the applied potential to the external lateral electrodes. Current conservation and an initial state of potential 0 were applied for all the layers. After, an adaptive physical controlled and extra fine mesh was applied. Finally, a frequency domain analysis at 1.7 kHz was performed. Thus, surface current density ( $ec.normJ$ ) of bacteria was obtained (Fig. 5. C and Fig. 5.D). From the analysis of the obtained simulations we could assure that in case of a single bacteria diluted on a buffer with a conductivity which varies from  $0.5 \cdot 10^{-3}$  S/m to  $2.5 \cdot 10^{-3}$  S/m, current density is 99.9% located outside the bacteria. Hence, measured impedance is totally related to sample buffer conductivity rather than bacteria concentration (Fig. 5.C.).

Controlling buffer conductivity to be stable and at the levels of Milli-Q water, around  $8.2 \cdot 10^{-5}$  S/m, current density is mainly located in the cell membrane (Fig. 5.D) and impedance variation related to the quantity of trapped bacteria.

Hence, when the cells' media is not controlled by cleaning processes, impedance variations are strongly related to changes in the conductivity of the media due to bacteria [50,51]. To solve this issue, which is not confronted in other works to the best of our knowledge, an automated periodic cleaning process was implemented as part of the device working protocol assuring a reliable impedance measurement.

In the resulting protocol the micro-fluidic chip was first filled with Milli-Q water media to obtain the threshold impedance measurement. Afterwards, a 50  $\mu$ l sample of *E. coli* were injected through a controlled valve to the micro-fluidic chip and trapped by DEP forces while flowing continuously at 10  $\mu$ l/min, higher flow rate compared with other solutions for DEP and IA combination, such as 2-4  $\mu$ l/min [30]. After each 50  $\mu$ l sample of bacteria was injected into the channel, 50  $\mu$ l of Milli-Q water, with a specified conductivity of  $8.2 \cdot 10^{-5}$  S/m, was automatically injected at 10  $\mu$ l/min to ensure a steady media conductivity for the impedance measurement. Once the Milli-Q water was injected, the impedance electronic module was activated and the DEP generator deactivated by means of multiplexor. 4 contiguous impedance measurements were performed each time in order to evaluate precision. Afterwards, another 50  $\mu$ l sample of *E. coli* was injected and the process repeated until all the samples were injected. So, the impedance measurement is always performed after each 50  $\mu$ l bacteria sample was injected, trapped and cleaned. The whole process were performed to scan the 500 Hz to 5 kHz IA frequency range each 100 Hz. The DEP was generated by applying two 15 Vpp counter phased signals through the inter-digitated electrodes. The results of the experimental impedance measurements for three frequencies (500, 1700 and 5000 Hz) are depicted in Fig. 6.

Results are depicted as the increment ( $\Delta|Z|=|Z|-|Z_0|$ ) between the different impedance magnitude measurements for every bacteria sample injected ( $|Z|$ ) and the initial media impedance magnitude measurement ( $|Z_0|$ ). Figure 6.A depicts  $\Delta|Z|$  measurements through time for the initial and final frequency value, 500 Hz and 5 kHz respectively, as well as the 1.7 kHz frequency  $\Delta|Z|$  measurements, which seems to be more sensitive and reliable with an accuracy

error of less than 2% of bacteria concentration with a correlation of 0.988 are represented. Precision can be evaluated with the coefficient of variation, which is the standard deviation of the 4 experiment repetitions divided by the mean value of the 4 repetitions measurement. The mean value of the coefficient of variation is 3.1% on the whole range, although the device is more precise for lower bacteria concentration levels where the coefficient of variation is below 3%.

Thus, steady and sensitive  $\Delta|Z|$  measurement at different frequencies, which is bacteria dependent, was observed. Furthermore, bioimpedance control of the achieved sample concentration showed a reliable sensitivity for the protocol including a bacteria cleaning step. The controlled and steady low media conductivity microenvironment solves issues regarding overall system viability.

The DEP module had a proven trapping efficiency of  $85.65 \pm 1.07$  %, for a single 50  $\mu\text{l}$  bacteria sample injected at continuous flow of 10  $\mu\text{l}/\text{min}$ , by measuring the escaped and the collected bacteria of a single load by cytometric analysis [40]. Although the whole process trapping efficiency had not been tested, each sample load was estimated to increment the bacteria concentration  $2 \cdot 10^8$  bacteria/mL inside the micro-fluidic chip. Figure 6.B depicts the  $\Delta|Z|$  measurements for each bacteria concentration increment (bacteria/ $\mu\text{L}$ ) when 1.7 kHz frequency is applied. However, our main goal was to verify that the process of bacterial concentration while monitoring the concentration is feasible, as it has been proved. The measured impedance values were related to the quantity of bacteria concentrated with a correlation of 0.988 and a coefficient of variation of 3.1%, avoiding distortion and instability related to undesired effects like media conductivity variations and DEP voltage interferences.

## 5. Concluding remarks

Here we describe a novel device and automated protocol, based on DEP and IA, to concentrate bacteria in bench-top setups. The system has been applied to concentrate *E. coli* and to automatically monitor its concentration. The electronic apparatus was validated using a micro-fluidic chip with 4 integrated gold electrodes specially designed for the application. The automated system was tested by trapping and measuring samples of *E. coli* 5K at a concentration of  $2 \cdot 10^7$  cells/mL. Concentration and real-time detection of the trapped bacteria inside the micro-fluidic chip was proven, working with a high flow rate injection of 10  $\mu\text{L}/\text{min}$ , using inter-digitated electrodes and any type of buffer conductivity [31, 32]. Bacteria buffer media conductivity, and its variability, was demonstrated to be a challenging issue to monitoring by means of IA. An automated protocol integrated in the overall system has been shown to solve this problem, strengthening the system versatility towards the use of different buffers. Before each measurement, the designed system cleans the bacteria samples periodically,

while trapped on the micro-fluidic chip, with Milli-Q water, with a controlled conductivity of  $8.2 \cdot 10^{-5}$  S/m. An automated system and protocol of bacteria injection, trapping, cleaning and short-time impedance measurement process has been designed using a single micro-fluidic chamber and custom instrumentation electronics. This is a useful tool, with which bacteria can be concentrated to given specifications while performing analytical procedures in biological labs. Moreover, the development of LoC DEP applications, removing the need of huge and expensive equipments, is an important research field aiming for smaller systems with better functionality, such as the integrated application specific integrated system (ASIC) stimulator for electrokinetically-driven micro-fluidic devices presented by Gomez-Quiñones et al. (2011) [52]. Nowadays, electronics technology allows to miniaturize devices such as the presented system. A SOI technology such as XTO18 from XFAB would be suitable to combine digital instrumentation and class E amplifiers inside a unique chip. However, some drawbacks must be considered when integrating the full system into the lab-on-a-chip device, as it would increase disposable cost or reduce applicability due to possible contaminations. Still, the simplicity of the presented micro-fluidic device and the development of the custom electronics on a single ASIC, along with an automated procedure protocol, pushes towards the development of robust and reliable LoC automated bacterial concentrator relying on DEP concentration and IA monitoring.

## **Acknowledgements**

This work was financially supported by the THERAEDGE Project (FP7-ICT-2007-216027), funded by the 'Information and Communication Technologies' programme under the 7th Research Framework Programme of the European Union. The Nanobioengineering group is supported by the Commission for Universities and Research of the Department of Innovation, Universities, and Enterprise of the Generalitat de Catalunya (2009 SGR 505). This work was supported by Obra Social “La Caixa”. CIBER-BBN is an initiative funded by the VI National R&D&i Plan 2008-2011, Iniciativa Ingenio 2010, Consolider Program, CIBER Actions and financed by the Instituto de Salud Carlos III with assistance from the European Regional Development Fund. This material is based upon work supported by the Botín Foundation, Santander, Spain.

## References

- [1] Pethig, R., *Biomicrofluidics* 2010, 4, 22811.
- [2] Sun, T., Morgan, H., *Microfluid. Nanofluidics* 2010, 8, 423–443.
- [3] Hamada, R., Takayama, H., Shonishi, Y., Mao, L., Nakano, M., Suehiro, J., *Sensors Actuators B Chem.* 2013.
- [4] Agarwal, S., Sebastian, A., Forrester, L. M., Markx, G. H., *Biomicrofluidics* 2012, 6, 24101–2410111.
- [5] Fatoyinbo, H. O., Hoettges, K. F., Hughes, M. P., *Electrophoresis* 2008, 29, 3–10.
- [6] Venkatanarayanan, A., Keyes, T. E., Forster, R. J., *Anal. Chem.* 2013, 85, 2216–22.
- [7] Xu, M., Luo, X., Davis, J. J., *Biosens. Bioelectron.* 2013, 39, 21–5.
- [8] Feldsine, P. T., Falbo-Nelson, M. T., Hustead, D. L., *J. AOAC Int.* 1994, 77, 58–63.
- [9] Pouch Downes, F., Ito, K., *Compendium of Methods for the Microbiological Examination of Foods*, 4th ed., American Public Health Association, 2001, p. 676.
- [10] Morgan, H., Green, N. G., *AC electrokinetics: colloids and nanoparticles*, Research Studies Press, 2003.
- [11] Pohl, H. A., *J. Appl. Phys.* 1951, 22, 869.
- [12] Chin, C. D., Linder, V., Sia, S. K., *Lab Chip* 2007, 7, 41–57.
- [13] Figeys, D., Pinto, D., *Anal. Chem.* 2000, 72, 330 A–335 A.
- [14] Stone, H. A., Stroock, A. D., Ajdari, A., *Annu. Mech.* 2004, 36, 381–411.
- [15] Lapizco-Encinas, B. H., Simmons, B. A., Cummings, E. B., Fintschenko, Y., *Anal. Chem.* 2004, 76, 1571–1579.
- [16] Braff, W. A., Pignier, A., Buie, C. R., *Lab Chip* 2012, 12, 1327–1331.
- [17] Gascoyne, P. R. C., Noshari, J., Anderson, T. J., Becker, F. F., *Electrophoresis* 2009, 30, 1388–1398.
- [18] Gascoyne, P., Mahidol, C., Ruchirawat, M., Satayavivad, J., Watcharasit, P., Becker, F. F., *Lab Chip* 2002, 2, 70–5.
- [19] Moon, H. S., Kwon, K., Kim, S. I., Han, H., Sohn, J., Lee, S., Jung, H. I., *Lab Chip* 2011, 11, 1118–1125.
- [20] Fatoyinbo, H. O., McDonnell, M. C., Hughes, M. P., *Biomicrofluidics* 2014, 8, 044115.



- [21] Zordan, M. D., Grafton, M. M. G., Acharya, G., Reece, L. M., Cooper, C. L., Aronson, A. I., Park, K., Leary, J. F., *Cytom. A* 2009, 75, 155–162.
- [22] Deisingh, A. K., Thompson, M., *Analyst* 2002, 127, 567–581.
- [23] Hahm, B.-K., Bhunia, A. K., *J Appl Microbiol* 2006, 100, 1017–1027.
- [24] Bohaychuk, V. M., Gensler, G. E., King, R. K., Wu, J. T., McMullen, L. M., *J Food Prot* 2005, 68, 2637–2647.
- [25] Hong, B.-X., Jiang, L.-F., Hu, Y.-S., Fang, D.-Y., Guo, H.-Y., *J Microbiol Methods* 2004, 58, 403–411.
- [26] Foudeh, A. M., Fatanat Didar, T., Veres, T., Tabrizian, M., *Lab Chip* 2012, 12, 3249–66.
- [27] Ramírez, N., Regueiro, A., Arias, O., Contreras, R., 1989, 31.
- [28] Dweik, M., Stringer, R. C., Dastider, S. G., Wu, Y., Almasri, M., Barizuddin, S., *Talanta* 2012, 94, 84–89.
- [29] Grossi, M., Lanzoni, M., Pompei, a, Lazzarini, R., Matteuzzi, D., Riccò, B., *Biosens. Bioelectron.* 2010, 26, 983–90.
- [30] Dastider, S.G., Barizuddin, S., Dweik, M., Almasri, M., *RSC Advances* 2013, 3, 26297–26306.
- [31] Park, S., Zhang, Y., Wang, T.-H., Yang, S., *Lab Chip* 2011, 11, 2893–2900.
- [32] Rozitsky, L., Fine, A., Dado, D., Nussbaum-Ben-Shaul, S., Levenberg, S., Yossifon, G., *Biomed. Microdevices* 2013, 15, 859–65.
- [33] Croxen, M. A., Law, R. J., Scholz, R., Keeney, K. M., Wlodarska, M., Finlay, B. B., *Clin Microbiol Rev* 2013, 26, 822–880.
- [34] Sievert, D. M., Ricks, P., Edwards, J. R., Schneider, A., Patel, J., Srinivasan, A., Kallen, A., Limbago, B., Fridkin, S., *Infect. Control Hosp. Epidemiol.* 2013, 34, 1–14.
- [35] Ulett, G. C., Totsika, M., Schaale, K., Carey, A. J., Sweet, M. J., Schembri, M. A., *Curr Opin Microbiol* 2013, 16, 100–107.
- [36] Dhama, K., Chakraborty, S., Tiwari, R., Verma, A. K., Saminathan, M., Amarpal, Y. S. M., Nikousefat, Z., Javdani, M., Khan, R. U., .
- [37] Sabounchi, P., Morales, A. M., Ponce, P., Lee, L. P., Simmons, B. A., Davalos, R. V., *Biomed. Microdevices* 2008, 10, 661–70.
- [38] Jones, T. B., *Electromechanics of particles*, Cambridge Univ Pr, 2005.
- [39] Castellarnau, M., Errachid, A., Madrid, C., Juárez, A., Samitier, J., *Biophys. J.* 2006, 91, 3937–3945.
- [40] Moral Zamora, B. del, *Micro Nanosyst.* 2014, 6.

- [41] Fairooz, T., Istya, S., *Int. J. Biol. Life Sci.* 2011.
- [42] Patterson, R., *Biomed. Eng. Handbook*, JD Bronzino, ... 2000.
- [43] Martinson, O. G., Grimnes, S., *Bioimpedance & Bioelectricity Basics* 2008.
- [44] Lenaerts, B., Puers, R., *Omnidirectional inductive powering for biomedical implants*, Springer, 2009.
- [45] Rasid, M. H., González, M. H. R. V., Fernández, P. A. S., *Electrónica de potencia: Circuitos, dispositivos y aplicaciones*, Pearson Educación, 2004.
- [46] Sokal, N. O., *QEX Commun.Quart* 2001, 9–20.
- [47] Cheng, M. S., Ho, J. S., Lau, S. H., Chow, V. T. K., Toh, C.-S., *Biosens Bioelectron* 2013, 47, 340–344.
- [48] Yang, L., *Talanta* 2008, 74, 1621–1629.
- [49] Punter-Villagrasa, J., Colomer-Farrarons, J., Miribel, P. L., Rinken, T. (Ed.), *Bioelectronics for Amperometric Biosensors*, Intech 2013. Available: <http://www.intechopen.com/books/state-of-the-art-in-biosensors-general-aspects/bioelectronics-for-amperometric-biosensors>
- [50] Varshney, M., Li, Y., *Biosens Bioelectron* 2009, 24, 2951–2960.
- [51] Li, M., Li, S., Cao, W., Li, W., Wen, W., Alici, G., *Microfluid. Nanofluidics* 2013, 14, 527–539.
- [52] Gomez-Quñones, J., Moncada-Hernández, H., Rossetto, O., Martinez-Duarte, R., Lapizco-Encinas, B.H., Madou, M., Martinez-Chapa, S.O. *New Circuits and Systems Conference (NEWCAS)*, 2011, 350–353

**Figures:**

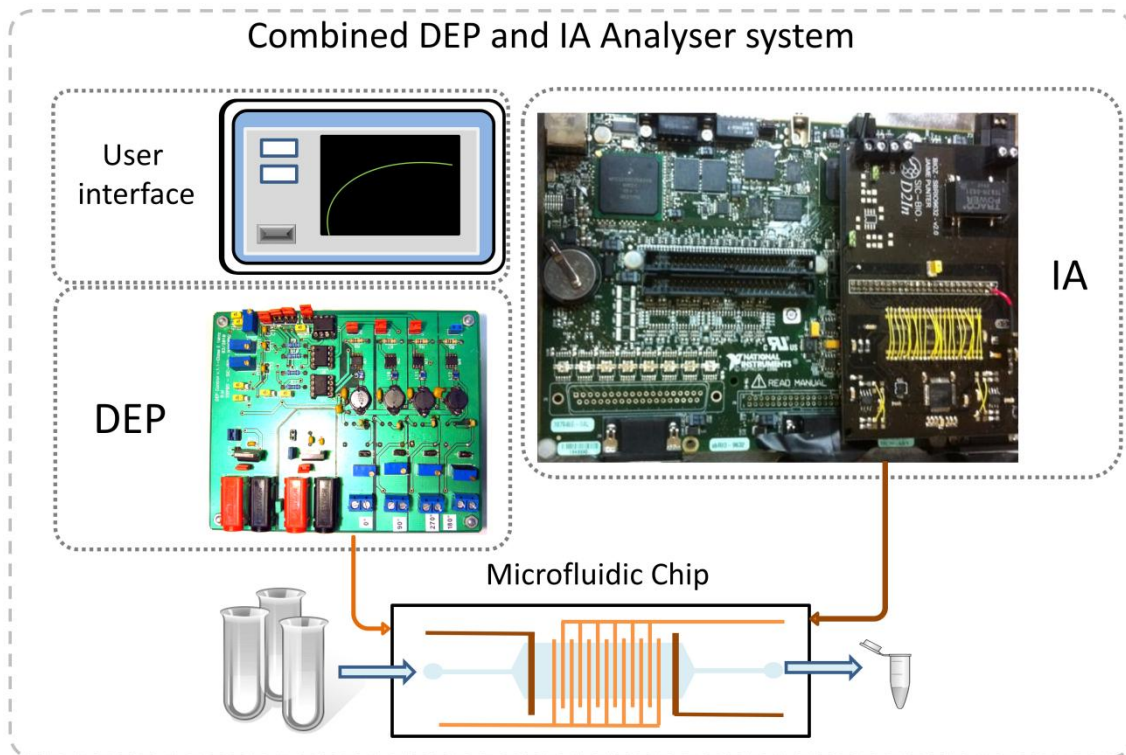


**Figure 1.** Combined system overview.

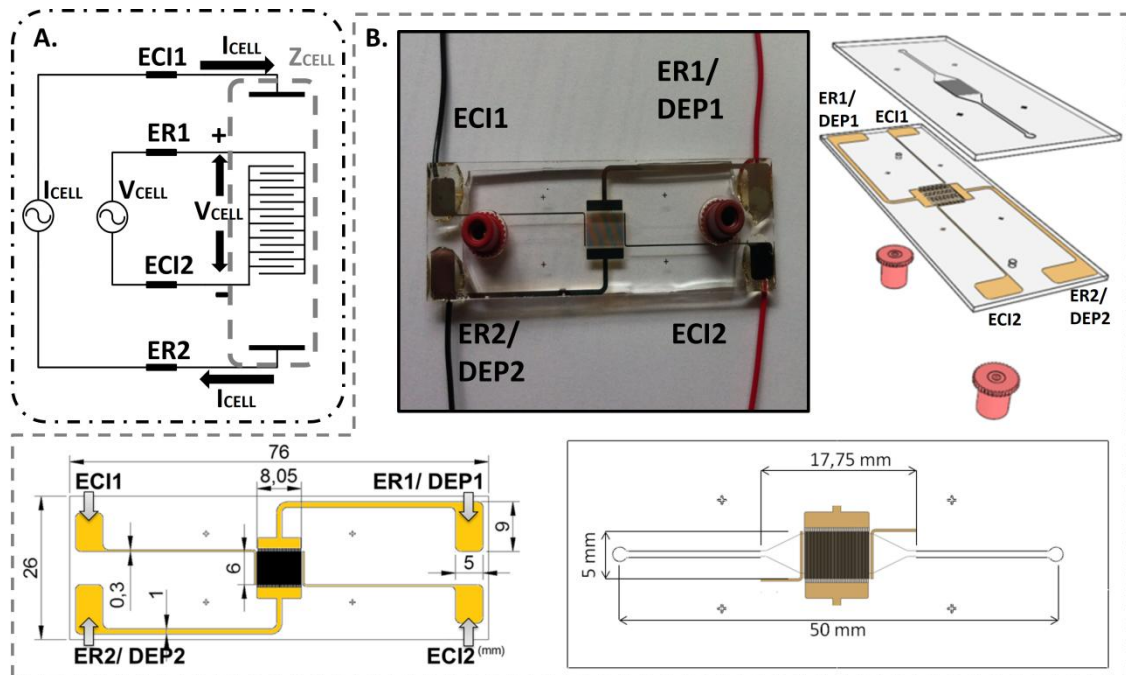


**Figure 2.** A: 4 electrode impedance measurement method. B: Designed micro-fluidic chip. ECI1-ECI2 are the current injection electrodes, ER1-ER2 are the reading electrodes and DEP1-DEP2 are referred to electrodes where DEP is applied.

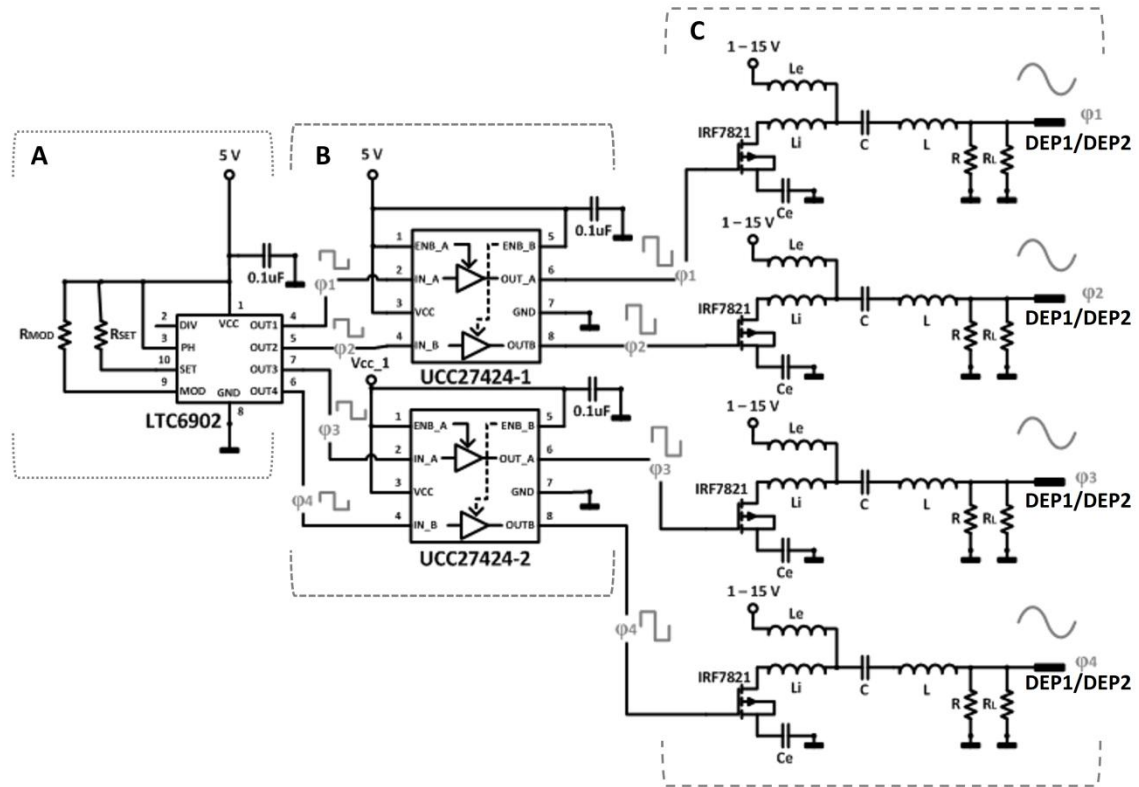


**Figure 3.** Schematic of the DEP module. A: Square signal generator. B: Power driver. C: Class E amplifier.

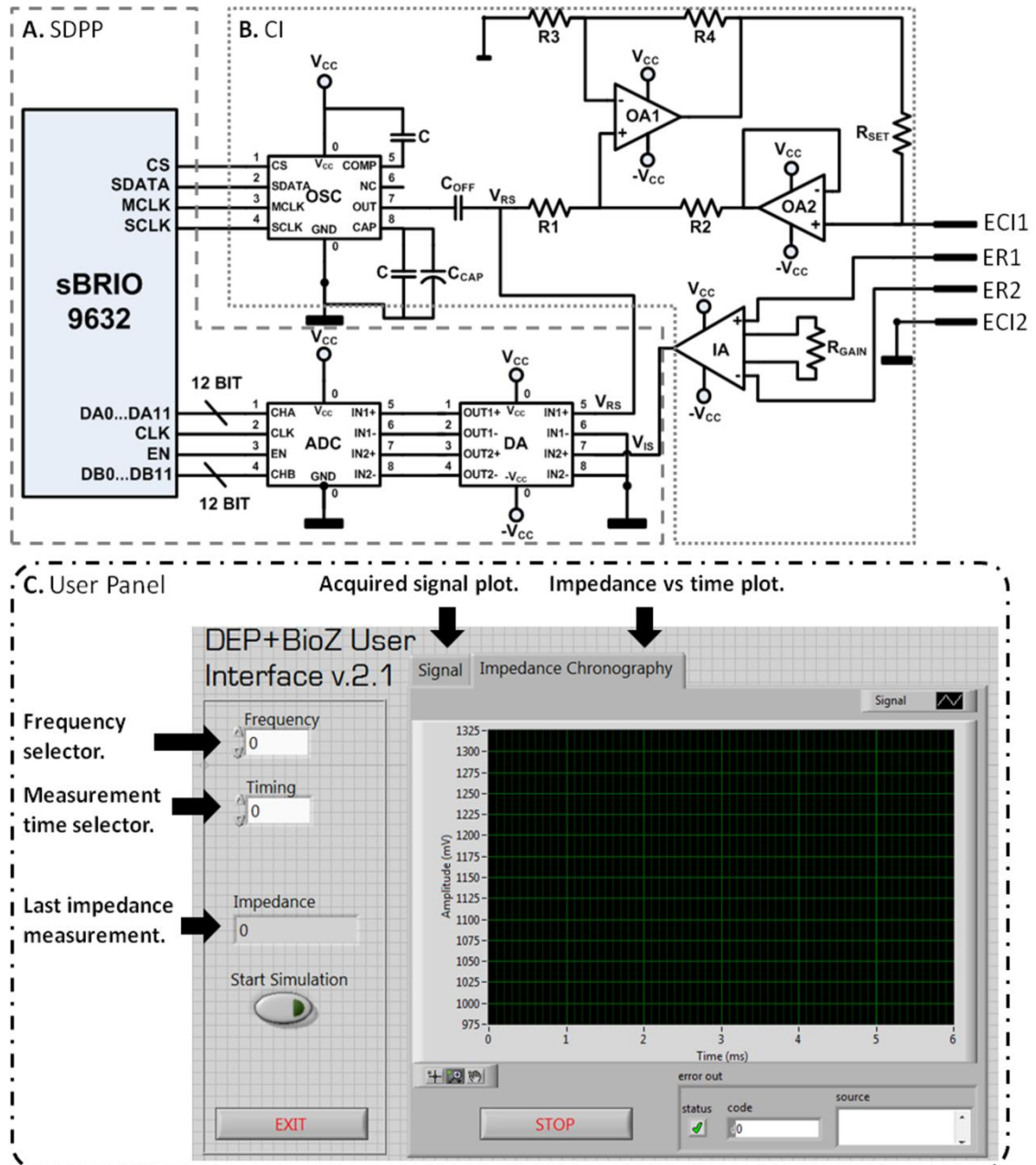


**Figure 4.** Schematic of the IA module. A: Signal Digitalization and Post-Processing module (SDPP). B: Current Injection Module (CI). C: Front-end user panel for experiments control and data displaying.

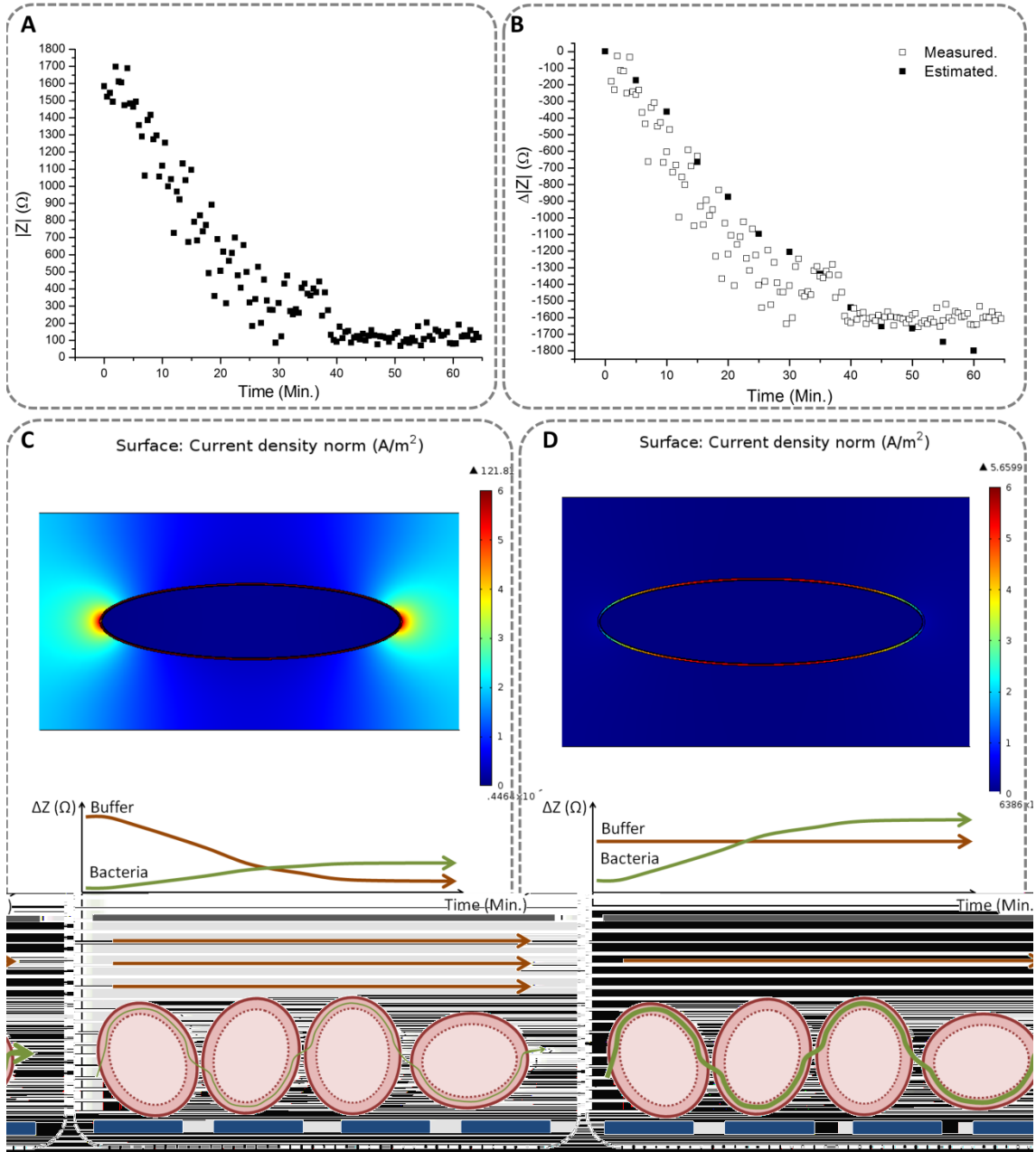


**Figure 5.** A: Impedance magnitude measured during the trapping operation. B: Experimental versus estimated impedance magnitude relative incremental changes. C: Comsol Multiphysics simulation of a single diluted cell on high conductivity buffer ( $0.5 \cdot 10^{-3}$  S/m to  $2.5 \cdot 10^{-3}$  S/m). Schematic modelization of current flow path and contribution to impedance measurement of both buffer and trapped bacteria. D: Comsol Multiphysics simulation of a single diluted cell on low conductivity steady buffer (Milli-Q water;  $8.2 \cdot 10^{-5}$  S/m). Schematic modelization of current flow path and contribution to impedance measurement of both buffer conductivity and trapped bacteria.

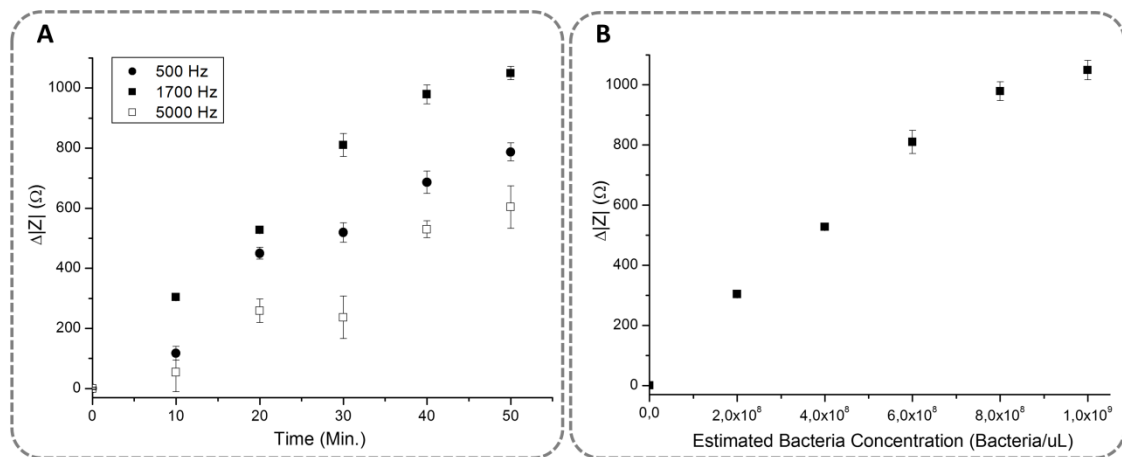


**Figure 6.** A: Impedance magnitude measured changes during bacterial sample on-chip concentration at several given times. Medium cleaning procedure was performed before each measurement. B: Impedance magnitude measurements at 1700 Hz related to estimated bacteria concentrations.